

# Formation of carbon-monoxide by radiative association: a quantum-dynamical study

Jan Franz<sup>1\*</sup>, Magnus Gustafsson<sup>1</sup> and Gunnar Nyman<sup>1</sup>

<sup>1</sup>*Department of Chemistry, University of Gothenburg, 41296 Gothenburg, Sweden*

Accepted 201X Month Day. Received 201X Month Day; in original form 201X Month Day

## ABSTRACT

Rate coefficients for the formation of carbon-monoxide (CO) by radiative association of carbon and oxygen atoms are computed using quantum dynamical simulations. At temperatures above 9 Kelvin CO radiative association is dominated by C(<sup>3</sup>P) and O(<sup>3</sup>P) approaching on the A<sup>1</sup>Π potential energy curve. The rate coefficient is estimated as  $k = A \left(\frac{T}{300K}\right)^\alpha \exp -\frac{\beta}{T}$  with  $A = 2.78 \times 10^{-18} \text{cm}^3 \text{s}^{-1}$ ,  $\alpha = -0.016$  and  $\beta = 92.2$  for temperatures between 6 and 127.2 Kelvin, and  $A = 2.73 \times 10^{-17} \text{cm}^3 \text{s}^{-1}$ ,  $\alpha = 0.41$  and  $\beta = 340$  for temperatures between 127.2 and 15000 Kelvin. Furthermore we computed the rate coefficients for approaching on the X<sup>1</sup>Σ<sup>+</sup> curve. For temperatures below 200 Kelvin it is between  $0.7 \times 10^{-22} \text{cm}^3 \text{s}^{-1}$  and  $4 \times 10^{-22} \text{cm}^3 \text{s}^{-1}$ .

**Key words:** atomic data – atomic processes – molecular data – molecular processes – ISM: molecules – supernova remnants.

## 1 INTRODUCTION

Radiative association of carbon-monoxide (CO) has been discussed in order to explain the abundance of CO in the inner ejecta of the supernova 1987A (Petuchowski et al. 1989; Gearhart et al. 1999; Hartquist and Williams 1995).

When a carbon and an oxygen atom collide, they can form a bound CO molecule by emitting energy as a photon  $\text{C}(\text{}^3\text{P}) + \text{O}(\text{}^3\text{P}) \rightarrow \text{CO}(\text{X}^1\Sigma^+) + h\nu$ .

The rates for this reaction are required at many different temperatures for modelling the CO-formation in different astrophysical environments (see e.g. (Prasad and Huntress 1980; Glover et al. 2010)).

Each of the two atoms, C and O, in their electronic ground state has nine spin-orbit states, which can form a total of  $9 \times 9 = 81$  molecular electronic states. These include two Σ<sup>+</sup> states, one Σ<sup>-</sup> state, two Π states and one Δ state, each of them with total electronic spin multiplicities singlet, triplet and quintet. Dalgarno et al. (1990) discuss the importance of the various states for CO formation by radiative association and give rough numerical estimates for the corresponding thermal reaction rate coefficients.

An early estimate for the radiative association rate coefficient for formation of CO is given by Julienne and Krauss (1973) as  $10^{-17} \text{cm}^3 \text{s}^{-1}$ , which is independent of the temperature. Later Dalgarno et al. (1990) and Singh et al. (1999) computed the rate constant from a semiclassical formalism using classical trajectories for temperatures above

300 Kelvin. Both groups of authors simulated the process in which the two reaction partners approach on the potential energy curve of the A<sup>1</sup>Π electronic state and radiate into the X<sup>1</sup>Σ<sup>+</sup> state. Dalgarno et al. (1990) and Singh et al. (1999) used the *ab initio* data of Cooper and Kirby (1987). In that study the potential energy curve of the A<sup>1</sup>Π state has a barrier of  $838 \text{cm}^{-1}$  (1200 Kelvin). The classical trajectories cannot penetrate into the reaction zone for collision energies below the barrier height and quantum mechanical tunneling becomes important. The importance of quantum mechanical tunneling for radiative association at low temperatures is pointed out by Bain and Bardsley (1972) and Smith (1989).

In this paper we present quantum dynamical cross sections and reaction rate coefficients for the formation of carbon-monoxide for the process in which the carbon and oxygen atom approach on the A<sup>1</sup>Π potential energy curve and radiate into the electronic ground state X<sup>1</sup>Σ<sup>+</sup>. The method employed treats the nuclear wavefunction quantum-mechanically and therefore takes full account of tunneling effects. Furthermore we present computations for the non-electronic transitions when the reactants approach on the potential energy curve of the electronic ground state X<sup>1</sup>Σ<sup>+</sup> and radiate into ro-vibrational levels of the same electronic state.

## 2 THEORY

The thermal rate constant (in  $\text{cm}^3 \text{s}^{-1}$ ) at a given temperature  $T$  to form the molecule in the electronic state

\* E-mail: [jan@theory.phys.ucl.ac.uk](mailto:jan@theory.phys.ucl.ac.uk) (JF)

$\eta'$  by radiative association from the initial electronic state  $\eta$  is given by (Zygelman and Dalgarno 1990)

$$k_{\eta\eta'}(T) = \left(\frac{8}{\mu_{\text{red}}\pi}\right)^{1/2} \left(\frac{1}{k_B T}\right)^{3/2} \times \int_0^\infty E \cdot \sigma_{\eta\eta'}(E) \cdot e^{-E/k_B T} dE .$$

Here  $\mu_{\text{red}}$  is the reduced mass,  $k_B$  is the Boltzmann constant and  $E$  is the collisional energy. The total integral cross section  $\sigma_{\eta\eta'}(E)$  for the radiative association process can be expressed as (see e.g. (Babb and Dalgarno 1995; Gianturco and Gori Giorgi 1996))

$$\sigma_{\eta\eta'}(E) = \sum_{v',J'} \sum_J \frac{64 \pi^5 \hbar^2}{3 c^3} \frac{\nu^3}{2\mu_{\text{red}}E} P_\eta S_{JJ'} M_{\eta EJ, \eta' v' J'}^2 ,$$

where the sum is over initial angular momenta  $J$  and all final vibrational states  $v'$  and rotational states  $J'$ .  $c$  is the speed of light,  $S_{JJ'}$  are the Hönl-London factors (Watson 2008), and  $\nu$  is the frequency of the emitted photon. The statistical weight factor  $P_\eta$  for approaching in the initial molecular electronic state  $\eta$  is given by (see e.g. Andreazza et al. (1995))

$$P_\eta = \frac{(2S_{\text{mol}} + 1)(2 - \delta_{0,\Lambda})}{(2L_C + 1)(2S_C + 1)(2L_O + 1)(2S_O + 1)} ,$$

where  $L_C$ ,  $S_C$ ,  $L_O$ ,  $S_O$ , are the electronic orbital and electronic spin of the carbon and oxygen atom,  $S_{\text{mol}}$  is the total electronic spin of the molecular electronic state, and  $\Lambda$  is the quantum numbers of the projections of the electronic angular momentum of the initial molecular electronic state  $\eta$  onto the molecular axis. For the  $X^1\Sigma^+ \leftarrow A^1\Pi$  transition we have  $P_\Pi = 2/81$  and for the  $X^1\Sigma^+ \leftarrow X^1\Sigma^+$  transition  $P_\Sigma = 1/81$ .  $M_{\eta EJ, \eta' v' J'}$  is given by the integral

$$M_{\eta EJ, \eta' v' J'} = \int_0^\infty F_{\eta EJ}(r) \mu_{\eta\eta'}(r) \Phi_{\eta' v' J'}(r) dr .$$

Here  $\mu_{\eta\eta'}(r)$  is the matrix element of the dipole moment operator between the two molecular electronic states  $\eta$  and  $\eta'$ , which depends on the internuclear distance  $r$ . In the case that the initial and final electronic state are the same  $\mu_{\eta\eta'}(r)$  is the electronic dipole moment, otherwise it is the electronic transition dipole moment. The wavefunction  $F_{\eta EJ}(r)$  is the time-independent continuum wavefunction of the initial electronic state  $\eta$  for the partial wave  $J$  and normalized to the collision energy  $E$  (see e.g. Taylor (2009)). The wavefunction  $\Phi_{\eta' v' J'}(r)$  is an eigenfunction for the potential energy curve of the final electronic state  $\eta'$  with quantum numbers  $v'$  and  $J'$  to indicate its vibrational and rotational levels.

### 3 COMPUTATIONAL DETAILS

#### 3.1 Computational Methods

The wavefunctions  $\Phi_{\eta' v' J'}(r)$  for the bound states are computed using discrete variable representation in the formulation of Colbert and Miller (1992). The continuum wavefunction  $F_{\eta EJ}(r)$  is computed by R-matrix propagation (Kulander and Light 1980; Stechel et al. 1978) as described in the appendix. We have used the following grid of energies: in

the energy interval  $1 \times 10^{-5} - 0.1$  eV we have used a step size of  $1 \times 10^{-5}$  eV, in the interval  $0.1 - 1.0$  eV a step size of  $1 \times 10^{-4}$  eV, and in the interval  $1.0 - 10.0$  eV a step size of  $1 \times 10^{-3}$  eV.

#### 3.2 Molecular Data

The potential energy curves, the transition dipole moments and the dipole moments are calculated with the internally-contracted multi-reference configuration interaction method using the aug-cc-pV6Z basis set as implemented in MOLPRO (Werner and Knowles 1988; Knowles and Werner 1988).

### 4 RESULTS

In this study we are considering the two lowest-lying electronic states  $X^1\Sigma^+$  and  $A^1\Pi$ . Radiative association can follow approach on any of the two electronic states and it can radiate into any of the two states. Therefore four different transition can occur, two transition ( $X^1\Sigma^+ \leftarrow X^1\Sigma^+$  and  $X^1\Sigma^+ \leftarrow A^1\Pi$ ) with the electronic ground state as final state and two transitions ( $A^1\Pi \leftarrow X^1\Sigma^+$  and  $A^1\Pi \leftarrow A^1\Pi$ ) with the first excited singlet state  $A^1\Pi$  as final electronic state. Dalgarno et al. (1990) mention the possibility of radiative association by following approach on the  $X^1\Sigma^+$  curve and radiating into the  $A^1\Pi$  state, but they give numerical estimates of the rate coefficient only for the  $X^1\Sigma^+ \leftarrow A^1\Pi$  transition.

In order to get a rough estimate of the importance of the two transitions ending in the  $A^1\Pi$ , we have done some initial computations using the potentials, dipole and transition dipole moments of Cooper and Kirby (1987) and Kirby and Cooper (1989). We have found that the computed rate coefficient for forming CO in the  $A^1\Pi$  state are several orders of magnitude smaller than the rate coefficients for forming CO in the  $X^1\Sigma^+$  state and therefore we did not re-compute them using our new potentials, dipole and transition dipole moments.

The cross section and hence the rate coefficient for the association by approaching on the  $A^1\Pi$  curve depends strongly on the barrier height on that surface. Our *ab initio* calculations give a barrier height of  $636 \text{ cm}^{-1}$ . This is in good agreement with a recent study by Varandas (2007), who reports a barrier height of  $594 \pm 46 \text{ cm}^{-1}$ . The previous studies on radiative association of CO by Dalgarno et al. (1990) and Singh et al. (1999) employed the *ab initio* data of Cooper and Kirby (1987). Cooper and Kirby (1987) report a barrier height of  $838 \text{ cm}^{-1}$ , which they obtain by interpolating their *ab initio* data. Their highest computed data point, however, lies at  $649 \text{ cm}^{-1}$ .

Figure 1 shows the computed total cross sections for forming CO in the  $X^1\Sigma^+$  state by approaching either on the  $A^1\Pi$  or  $X^1\Sigma^+$  curve. The cross section for the  $X^1\Sigma^+ \leftarrow A^1\Pi$  transition increases significantly at collision energies between 5 meV and 70 meV. Since the barrier height is 79 meV ( $636 \text{ cm}^{-1}$ ), this increase is due to tunneling through the barrier. The baseline of the cross section for approaching on the  $X^1\Sigma^+$  curve is nearly constant with respect to the collision energy. It has a large number of resonances, some

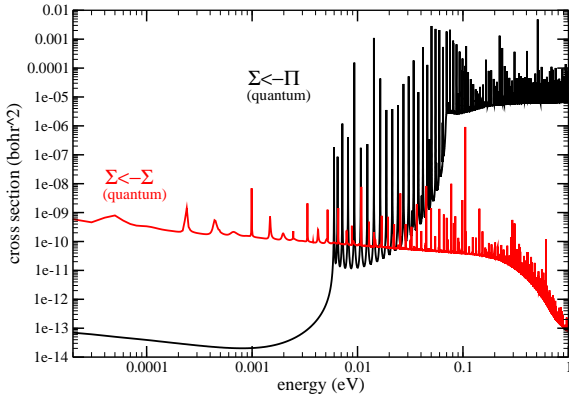


**Figure 1.** Computed total cross sections for forming CO in the  $X^1\Sigma^+$  state by approaching on the  $X^1\Sigma^+$  curve (red) and on the  $A^1\Pi$  curve (black).

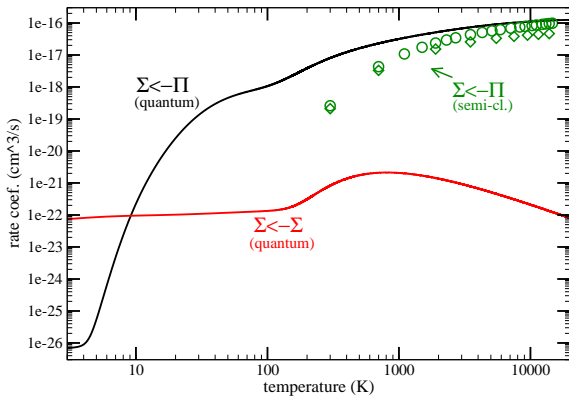


**Figure 2.** Computed reaction rates for forming CO in the  $X^1\Sigma^+$  state by approaching on  $X^1\Sigma^+$  curve (red) or on the  $A^1\Pi$  curve (black); semi-classical results by Singh et al. (1999) (green circles) and Dalgarno et al. (1990) (green diamonds).

of them having heights two orders of magnitude higher than the base line.

The computed reaction rates for the two transitions are shown in figure 2 together with the semi-classical results of Dalgarno et al. (1990) and Singh et al. (1999). At temperatures below 900 Kelvin our computed reaction rates are about one order of magnitude larger than predicted by the semi-classical methods. Even at temperatures as low as 100 Kelvin, the reaction rate is above  $10^{-18} \text{ cm}^3 \text{ s}^{-1}$ . For higher temperatures the agreement between the quantum dynamical and the semi-classical rates is better.

The total reaction rate for radiative association

$$k(T) = k_{AX}(T) + k_{XX}(T)$$

is the sum of the reaction rates  $k_{AX}$  and  $k_{XX}$  for the  $X^1\Sigma^+ \leftarrow A^1\Pi$  transition and the  $X^1\Sigma^+ \leftarrow X^1\Sigma^+$  transition respectively. Each rate-coefficient curve shown in figure 1 can be approximated by a three parameter curve using a range of temperature intervals (Kooij 1893)

$$k = A \left( \frac{T}{300K} \right)^\alpha \exp -\frac{\beta}{T}.$$

The fitting parameters for the two reaction rates are given in table 1. On average the analytic form reproduces the plotted

data within 1 per cent. However large relative errors can be found at the temperatures at which the parameters are switched from one temperature interval to the other. Hence the largest relative error for the  $X^1\Sigma^+ \leftarrow A^1\Pi$  transition is 18 per cent and can be found at 127.2 Kelvin. For the  $X^1\Sigma^+ \leftarrow X^1\Sigma^+$  the largest relative error (18 per cent) is at the temperature 144.1 K.

## 5 CONCLUSIONS

The rate coefficients for forming CO by radiative association of carbon and oxygen atoms has been estimated using quantum dynamical simulations. Compared to previous semi-classical simulations by Dalgarno et al. (1990) and Singh et al. (1999) our simulations predict much higher rate coefficients for temperatures below 900 Kelvin, where quantum mechanical tunneling is important.

While at temperatures above 9 Kelvin CO is mainly formed by  $C(^3P)$  and  $O(^3P)$  approaching on the  $A^1\Pi$  potential energy curve, at temperatures below 9 Kelvin approaching on the  $X^1\Sigma^+$  potential energy curve becomes the dominant process. The rate at those temperatures is, however, very small.

The total rate coefficient is expressed as a sum of the rate coefficients for two processes. The rate coefficients are fitted to the three parameter expression  $k = A \left( \frac{T}{300K} \right)^\alpha \exp -\frac{\beta}{T}$ , with the parameters given in table 1.

## ACKNOWLEDGMENTS

This project was supported by the ASTRONET CATS collaboration. Furthermore the authors thank the Chalmers C3SE computer center for computer support.

## REFERENCES

- Andreazza C. M., Singh P. D., Sanzovo G. C. 1995, ApJ, 451, 889
- Babb J. F., Dalgarno A. 1995, Phys. Rev. A, 51, 3021
- Bain R. A., Bardsley J. N. 1972, J. Phys. B: At. Mol. Phys., 5, 275
- Batista V. M. O., Rodrigues S. P. J., Varandas A. J. C. 2007, Asian J. Spectrosc., 11, 133
- Colbert D. T., Miller W. H. 1992, J. Chem. Phys., 96, 1982
- Cooper D. L., Kirby K. 1987, J. Chem. Phys., 87, 424
- Dalgarno A., Du M. L., You J. H. 1990, ApJ, 349, 675
- Gearhart R. A., Wheeler J. C., Swartz D. A. 1999, ApJ, 410, 944
- Gianturco F. A., Gori Giorgi P. 1996, Phys. Rev. A, 54, 4073
- Glover S. C. O., Federrath C., Mac Low M.-M., Klessen R. S. 2010, MNRAS, 404, 2
- Hartquist T. W., Williams D. A. 1995, The Chemically Controlled Cosmos. Cambridge University Press, Cambridge
- Julienne P. S., Krauss M. 1973, in Gordon M. A., Snyder L. E., eds, , Molecules in the Galactic Environment. John Wiley and Sons, New York, pp 353–374
- Kirby K., Cooper D. L. 1989, J. Chem. Phys., 90, 4895

**Table 1.** Parameters from fitting the reaction rates to the three-parameter expression  $k = A \left( \frac{T}{300K} \right)^\alpha \exp -\frac{\beta}{T}$ .

transition	temp. range	$A/\frac{\text{cm}^3}{\text{s}}$	$\alpha$	$\beta/K$
$X^1\Sigma^+ \leftarrow A^1\Pi$	6 – 127.2 K	$2.78 \times 10^{-18}$	-0.016	92.2
$X^1\Sigma^+ \leftarrow A^1\Pi$	127.2 – 15000 K	$2.73 \times 10^{-17}$	0.41	340
$X^1\Sigma^+ \leftarrow X^1\Sigma^+$	3 – 144.1 K	$1.61 \times 10^{-22}$	0.17	-0.12
$X^1\Sigma^+ \leftarrow X^1\Sigma^+$	144.1 – 361.4 K	$3.70 \times 10^{-21}$	0.10	458
$X^1\Sigma^+ \leftarrow X^1\Sigma^+$	361.4 – 15000 K	$4.11 \times 10^{-20}$	-1.47	1223

Knowles P. J., Werner H.-J. 1988, Chem. Phys. Lett., 145, 514

Kooij D. M. 1893, Z. Phys. Chem., 12, 155

Kulander K. C., Light J. C. 1980, J. Chem. Phys., 73, 4337

Petuchowski S. J., Dwek E., Allen Jr. J. E., Nuth J. A., 1989, ApJ, 342, 406

Prasad S. S., Huntress Jr. W. T. 1980, ApJ Suppl., 43, 1

Simmons J. D., Bass A. M., Tilford S. G. 1969, ApJ, 155, 345

Singh P. D., Sanzono G. C., Borin A. C., Ornellas F. R. 1999, MNRAS, 303, 235

Smith I. W. M. 1989, ApJ, 347, 282

Stechel E. B., Walker R. B., Light J. C. 1978, J. Chem. Phys., 69, 3518

Taylor, J. R. 2009, Scattering Theory: The Quantum Theory of Nonrelativistic Collisions. Dover Publications, New York

Varandas A. J. C. 2007, J. Chem. Phys., 127, 114316

Watson J. K. G. 2008, J. Mol. Spectrosc., 252, 5

Werner H.-J., Knowles P. J. 1988, J. Chem. Phys., 89, 5803

Zygelman B., Dalgarno A. 1990, ApJ, 365, 239

This paper has been typeset from a  $\text{\TeX}$ / $\text{\LaTeX}$  file prepared by the author.

## APPENDIX A: COMPUTATION OF THE CONTINUUM WAVEFUNCTION

The continuum wavefunction  $F_{\eta EJ}(r)$  is computed by solving the radial Schrödinger equation by R-matrix propagation (see e.g. Kulander and Light (1980)). Since our equations do not contain any couplings between different reaction channels, we use a different expression for the radial wavefunction than the one derived in Kulander and Light (1980). In the following we suppress the indices  $\eta$ ,  $E$  and  $J$ . The radial wavefunction  $F_n = F(r_n)$  at the radial grid-point  $r_n$  is generated from the wavefunction at the point  $r_{n-1}$  by the recursion relation

$$F_n = - \left( 1 - \mathbf{r}_1^{(n)} \mathbf{R}_n^{-1} \right)^{-1} \mathbf{r}_2^{(n)} \mathbf{R}_{n-1}^{-1} F_{n-1} . \quad (\text{A1})$$

Here  $\mathbf{R}_n$  and  $\mathbf{R}_{n-1}$  are the global  $R$ -matrices at the radial grid point  $r_n$  and  $r_{n-1}$ , respectively, and  $\mathbf{r}_1^{(n)}$  and  $\mathbf{r}_2^{(n)}$  are the sector  $R$ -matrices at  $r_n$ . The elements of the sector  $R$ -matrices are given by (Stechel et al. 1978)

$$\mathbf{r}_1^{(n)} = \begin{cases} |\lambda_n|^{-1} \coth |h_n \lambda_n|, & \lambda_n^2 > 0 \\ -|\lambda_n|^{-1} \cot |h_n \lambda_n|, & \lambda_n^2 \leq 0 \end{cases} \quad (\text{A2})$$

$$\mathbf{r}_2^{(n)} = \begin{cases} |\lambda_n|^{-1} \operatorname{csch} |h_n \lambda_n|, & \lambda_n^2 > 0 \\ -|\lambda_n|^{-1} \operatorname{csc} |h_n \lambda_n|, & \lambda_n^2 \leq 0, \end{cases} \quad (\text{A3})$$

where  $h_n = r_n - r_{n-1}$  and  $\lambda_n^2 = 2\mu_{red}(V(r_n - \frac{h_n}{2}) - E)$ .